Water Research 247 (2023) 120746

Contents lists available at ScienceDirect

Water Research

journal homepage: www.elsevier.com/locate/watres

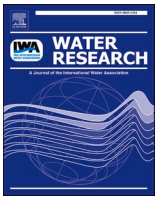

A probabilistic-deterministic approach for assessing climate change effects on infection risks downstream of sewage emissions from CSOs

J. Derx [a,1,2], H. Müller-Thomy [a,b,*,2], H.S. Kılıç [a,1], S. Cervero-Arago [c,1], R. Linke [d,1], G. Lindner [a,c,1], J. Walochnik [e], R. Sommer [c,1], J. Komma [a], A.H. Farnleitner [d,f,1], A.P. Blaschke [a,1]

[a] Institute of Hydraulic Engineering and Water Resources Management, TU Wien, Vienna, Austria
[b] Leichtweiß Institute for Hydraulic Engineering and Water Resources, Department of Hydrology and River Basin Management, Technische Universität Braunschweig, Brunswick, Germany
[c] Institute for Hygiene and Applied Immunology, Unit Water Hygiene, Medical University of Vienna, Vienna, Austria
[d] Research Group Microbiology and Molecular Diagnostics, Institute of Chemical, Environmental and Bioscience Engineering, TU Wien, Austria
[e] Molecular Parasitology, Institute of Specific Prophylaxis and Tropical Medicine, Medical University of Vienna, Austria
[f] Division Water Quality and Health, Department of Pharmacology, Physiology and Microbiology, Karl Landsteiner University of Health Sciences, Krems/Donau, Austria

ARTICLE INFO

Keywords:
Climate change
Rainfall disaggregation
Combined sewer overflow
QMRA
Infection risk
Reference pathogens

ABSTRACT

The discharge of pathogens into urban recreational water bodies during combined sewer overflows (CSOs) pose a potential threat for public health which may increase in the future due to climate change. Improved methods are needed for predicting the impact of these effects on the microbiological urban river water quality and infection risks during recreational use. The aim of this study was to develop a novel probabilistic-deterministic modelling approach for this purpose building on physically plausible generated future rainfall time series. The approach consists of disaggregation and validation of daily precipitation time series from 21 regional climate models for a reference period (1971–2000, C20), a near-term future period (2021–2050, NTF) and a long-term future period (2071–2100, LTF) into sub-daily scale, and predicting the concentrations of enterococci and *Giardia* and *Cryptosporidium*, and infection risks during recreational use in the river downstream of the sewage emissions from CSOs. The approach was tested for an urban river catchment in Austria which is used for recreational activities (i.e. swimming, playing, wading, hand-to-mouth contact). According to a worst-case scenario (i.e. children bathing in the river), the 95th percentile infection risks for *Giardia* and *Cryptosporidium* range from 0.08 % in winter to 8 % per person and exposure event in summer for C20. The infection risk increase in the future is up to 0.8 $\log_{10}$ for individual scenarios. The results imply that measures to prevent CSOs may be needed to ensure sustainable water safety. The approach is promising for predicting the effect of climate change on urban water safety requirements and for supporting the selection of sustainable mitigation measures. Future studies should focus on reducing the uncertainty of the predictions at local scale.

1. Introduction

Microbial safety of urban rivers is of paramount importance for public health when used for recreation, drinking water production or irrigation. Heavy rainfall events resulting in combined sewer overflows (CSOs) impair the quality of receiving waters through the discharge of waterborne pathogens such as the reference pathogens *Giardia* and *Cryptosporidium* (DeSilva et al., 2016; Feng and Xiao 2011) posing a potential public health risk when people are exposed during recreational activities (i.e. splashing, wading, hand-to-mouth contact of playing children). Such events are therefore often associated with waterborne infections according to reviews by Semenza (2020) and Guzman et al. (2015). This problem is likely to increase due to climate change leading to more extreme precipitation events worldwide (Bürger et al., 2021; Christensen and Christensen, 2003; Trenberth 2011). Appropriate and timely risk communication is critical for effective adaptation

* Corresponding author.
E-mail address: h.mueller-thomy@tu-braunschweig.de (H. Müller-Thomy).
[1] Interuniversity Cooperation Centre Water & Health (www.waterandhealth.at)
[2] Contributed equally to this work.

https://doi.org/10.1016/j.watres.2023.120746
Received 8 March 2023; Received in revised form 6 October 2023; Accepted 16 October 2023
Available online 17 October 2023

management (Cardona et al., 2012). The effects of climate change on CSO discharges, and the chemical and microbiological water quality of receiving waters have been studied in the past empirically or by means of urban hydrological modelling (Abtellatif et al., 2015; Gooré Bi et al. 2015; Jalliffier-Verne et al., 2015; Sterk et al., 2016; Gogien et al., 2022). For modelling the urban hydrological processes during CSOs, input rainfall data are required at high temporal resolutions due to the limited storage effects and the quick rainfall-runoff transformation, as demonstrated by Schilling (1991), Ochoa-Rodriguez et al. (2015), and references therein. On top of that, rainfall intensities can increase stronger at sub-daily than at daily temporal resolution, as found e.g. by Burn and Taleghani (2013) for a Canadian study area, and by Bürger et al. (2021) and Berg et al. (2013) for German regions. Rainfall time series from climate models, however, are generally available only at daily time steps. For disaggregating the rainfall time series, several methods were proposed such as the rectangular pulse model (Koutsoyiannis and Onof, 2001) and the method-of-fragments (Breinl and Di Baldassarre, 2019; Gogien et al., 2022). A more promising method which has not been applied in this context is the micro-canonical cascade model (Olsson, 1998). It considers the scaling behaviour of the rainfall process, which is assumed to be stationary over time and not affected by climate change, and exactly keeps the daily total amounts of rainfall during disaggregation. Another important advantage of the cascade model is the generation of continuous rainfall time series. This enables analysing e.g. the impact of complex long-lasting rainfall events with nested convective events in contrast to events with selected durations and return periods of rainfall.

Despite of this, most studies investigating the impacts of climate change on the water quality downstream of sewage emissions from CSOs used future precipitation data at daily temporal resolution as input, often relying on strongly simplified assumptions (Jalliffier-Verne et al., 2015; Gooré Bi et al. 2015). For example, Jalliffier-Verne et al. (2015) estimated loads of the faecal indicator bacteria *E. coli* into rivers via CSOs based on projected daily precipitation data available from regional climate models. The authors acknowledged that large uncertainties were involved in the predicted microbial loads due to a lack of local precipitation data for the future. Likewise, Gooré Bi et al. (2015) studied the impact of future climate on rainfall extreme values and loads of total suspended solids, organic and metal tracers, by adding a uniform increase of 20 % to the maximum observed 5 min rainfall intensity following guidelines of the Canadian government (MDDEFP 2013). The physical plausibility and the return periods of the constructed events of the above listed studies can be questioned, as the overall event characteristics such as the duration and the total rainfall amount remained unchanged. Only few modelling studies exist so far on the effects of global changes on the microbiological water quality and waterborne pathogen infection risks downstream of sewage emissions from CSOs (Jalliffier-Verne et al., 2017; Sterk et al., 2016). Jalliffier-Verne et al., 2017 considered an increase in concentrations of *E. coli* in CSO water as a consequence of population growth leading to a higher load of sewage. The authors, however, did not account for an increase in rainfall amounts or CSOs. In contrast, Sterk et al. (2016) transformed reference rainfall data according to changes under selected climate scenarios to study the effects on the bathing water infection risks downstream of sewage emissions from CSOs.

There is thus an urgent need for re-evaluating the impact of climate change on the microbiological water safety downstream of the sewage emissions from CSOs based on a correct representation of the rainfall processes as the major driver. The aim of this study was to develop a novel probabilistic-deterministic modelling approach for predicting the future changes in concentrations of faecal indicators (enterococci) and reference pathogens (*Giardia* and *Cryptosporidium*) in an urban river downstream of sewage emissions and the infection risks during recreational use (i.e. splashing, wading, hand-to-mouth contact of playing children). The approach builds on generated disaggregated future rainfall time series at sub-daily scale using the enhanced micro-canonical cascade model by Müller and Haberlandt (2018, Section 3.1). We tested the approach for a hypothetical urban drainage system aligned to the local conditions of an urban river catchment in Vienna, Austria.

2. Study area and data

2.1. Rainfall, water quantity data and exposure types

The study area is a river catchment in Vienna, Austria, inhabiting approximately 148,000 people (Fig. 1). The study area is classified as cold climate without dry season but warm summers according to the Köppen-Geiger climate classification (Peel et al., 2007). Rainfall data were available every 5 min for the years 2012–2020 (stations P1 – P5). The mean observed annual precipitation in the area was 770 mm during 2012–2017. The event-based and continuous rainfall characteristics are summarised in Table 1. The river originates west of Vienna and receives discharges from several tributaries. The river flow discharges at the river gauge range from 0.1 to 60 m^3/s with a mean of 1.8 m^3/s during 2012–2017. The river levels respond quickly to storm events with a response time of less than 30 min. The river is fed primarily from runoff from urban and forested flysch areas. The households in the urban hydrological model area (Fig. 1) are connected to a combined sewer system. The average dry weather wastewater flow from the catchment area is 0.65 m^3/s (Wien Kanal, personal communication). CSOs occur during times when the amount of rainfall and wastewater exceeds the storage capacity. There are several locations where CSOs can discharge into the river upstream the river gauge. These are connected to the urban sewer system which pipes the sewage water mixed with rain water towards the WWTP (Fig. 1). CSO discharges were measured directly upstream of the river gauge from June to September 2020. Water pressure transducers were installed next to the overflow wall and the discharges were estimated based on the formula of Poleni. Nine CSO events were observed in total.

Although the river is not an official bathing site, it is a popular recreational site throughout the year, and is also used for swimming in particular during summer. People can be exposed more or less throughout the year, e.g. via hand-to-mouth contact during playing, wading, biking in the river or when walking dogs taking baths in the river.

2.2. Climate scenarios

For climate impact analysis we used the bias-corrected ÖKS15-projections (Chimani et al., 2018; CCCA, 2020). The ÖKS15-projections are based on the regional climate models (RCM) of the EURO—CORDEX initiative, which are based on global climate models (GCM) within the CMIP5 initiative (Taylor et al., 2012). The ÖKS15-projections include 13 combinations of GCM and RCM for both scenarios, RCP4.5 and RCP8.5. From these 26 GCM-RCM combinations, two combinations of MOHC—HadGEM_CLM were removed due to pronounced underestimations of rainfall, especially in Eastern Austria which is where the study area is located (Chimani et al., 2018). Two more GCM-RCM combinations (MOHC—HadGEM_RCA) and one EC-Earth combination (EC-EARTH_CLMcom) were removed due to inconsistencies in the time series, i.e. the 31st of each month was missing. The resulting 21 GCM-RCM combinations were applied in this study (listed in the supplementary material S1). Although the climate data is provided with a technical raster width of 1 km, the true resolution is represented by a raster width of 12.5 km. For each rain station, the time series of the containing raster cell was extracted for a reference period (1971–2000, C20), a near-term future period (2021–2050, NTF) and a long-term future period (2071–2100, LTF). These climate scenario time series are from here on referred to as the respective rainfall stations P1 – P5.

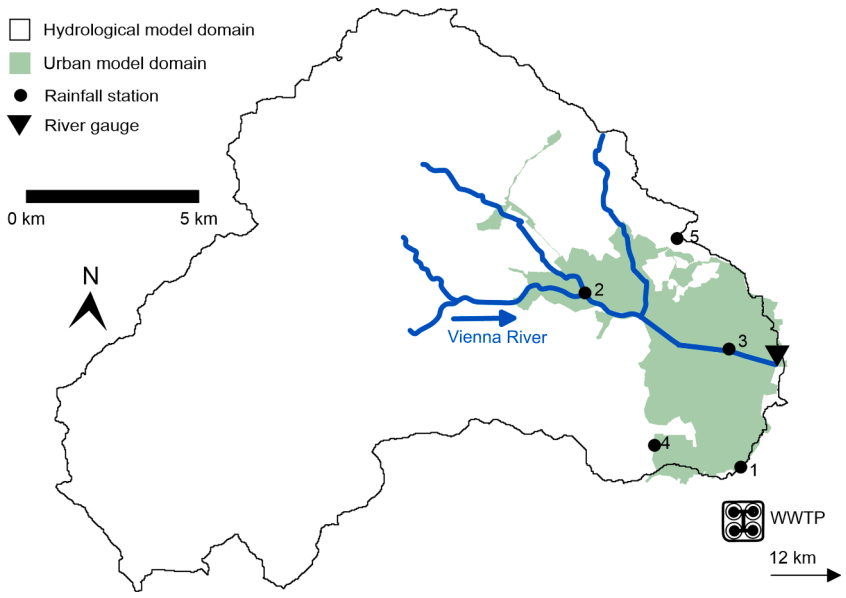

Fig. 1. Study area with hydrological and urban hydrological model domain and location of the rainfall stations, the river gauge and the WWTP collecting the wastewater mixed with rain water from the area.

Table 1
Event-based and continuous rainfall characteristics based on the 5-minute observed rainfall time series during 2012–2017 in the study area.

Rainfall station	Station-ID	Average intensity [mm/5 min]	Average wet spell amount [mm]	Average wet spell duration [min]	Average dry spell duration [min]	Probability of zero precipitation [%]
P1	LS3–21	0.2	0.4	11.1	286.9	96.3
P2	LWS-03	0.2	0.5	13.6	341.7	96.4
P3	LWS-22	0.2	0.4	11.6	302.3	96.3
P4	RWS-11	0.2	0.4	11.4	296.9	96.3
P5	RH1–15	0.2	0.4	12.2	342.2	96.7

3. Probabilistic-deterministic modelling approach

The modelling approach for predicting the impact of climate change on the concentrations of faecal indicators (enterococci) and reference pathogens (*Giardia* and *Cryptosporidium*) in the river downstream of the sewage emissions from CSOs and the infection risks associated with recreational use (section 2.1) consists of the following steps (outlined in Fig. 2):

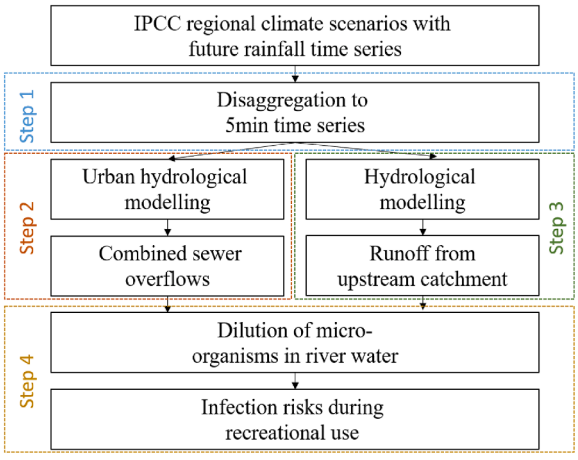

Fig. 2. Methodological steps and resulting data sets to analyse the impact of climate change on the microbiological river water quality and pathogen infection risks during recreational use downstream of sewage emissions from CSOs.

1) Rainfall disaggregation and validation of the rainfall time series from 21 GCM-RCM combinations for C20, NTF and LTF periods (Section 2.2) from daily into 5-minute intervals using the micro-canonical cascade model of Müller and Haberlandt (2018), an enhanced version of the original cascade model (Olsson, 1998, Section 3.1).
2) Prediction of the CSO volumes and frequencies, and concentrations of enterococci, *Giardia* and *Cryptosporidium* in CSO water using the disaggregated time series from step 1 as input for an urban hydrological model (US EPA SWMM5.1, Rosmann, 2015, Section 3.2).
3) Prediction of the river runoff using the disaggregated rainfall time series from step 1 as input for a distributed conceptual rainfall-runoff model (Blöschl et al., 2008; Section 3.3).
4) The results from steps 2 and 3 serve as input for modelling the dilution of enterococci, *Giardia* and *Cryptosporidium* in river water and the infection risks during recreational use (Sections 2.1 and 3.4).

To provide insights into the spatial component of the climate change effects, we used rainfall time series for each station P1 – P5 in step 1 (Fig. 1). In steps 2–4 we narrowed down the analysis to one rainfall station (P3) focusing on the temporal components.

3.1. Rainfall disaggregation and validation

To increase the temporal resolution Δt of the rainfall time series from the climate projections (Section 2.2), daily time steps are disaggregated to 5 min time steps using a micro-canonical cascade model according to Müller and Haberlandt (2018). The cascade model is applied due to its performance in previous studies (e.g. Müller and Haberlandt, 2015, Müller-Thomy, 2019, 2020). The basic principle is the self-similarity of neighbouring temporal scales, which enable conclusions from rainfall

intensities on a coarse scale on realistic rainfall intensity distribution on the neighbouring finer scale. This self-similarity is comprised in the cascade model parameters, which are estimated data-driven by aggregation of the observed 5 min precipitation time series at the five recording stations during 2012–2017 (Fig. 1). In Fig. 3, the general scheme of the cascade model is illustrated, disaggregating one coarse time step into b finer time steps of equal duration, where b is the branching number. While in the first disaggregation step $b = 3$ is applied (Δt: 24 h → 8 h), $b = 2$ is used throughout the subsequent disaggregation steps (Δt: 8 h → 4 h → 2 h → 1 h → 0.5 h → 0.25 h → 7.5 min). To achieve $\Delta t = 5$ min a linear transformation is applied. For the splitting, the weights W1 and W2 are used to determine the rainfall volume in the two fine time steps. The sum of W1 and W2 is 1 in each split, so that the rainfall volume is conserved exactly. An aggregation of the disaggregated rainfall would result in the same time series that has been used for the disaggregation. Possible combinations of W1 and W2 are given in (1), the so-called cascade-generator:

$$W_1, W_2 = x \; and \; 1 - x; 0 \leq x \leq 1 \tag{1}$$

P is the probability of each combination of weights. The probability P (0/1) e.g. denotes a splitting with no rainfall volume assigned to the first time step (W_1) and 100 % of the rainfall volume (W_2 =1 - W_1) in the second time step. The variable x is the relative fraction of rainfall assigned to the first time step. Considering x as a random variable for all disaggregation steps, a probability density function f(x) with the empirical probabilities for each value of x is estimated. Four different position classes that are assigned to each time step of the time series (starting, enclosed, isolated, ending) and two volume classes for each position are used. The mean of all rainfall intensities of the current cascade level (e.g. for $\Delta t = 4$ h) for one position was used as an acceptable threshold for this differentiation. For a detailed description of the cascade model we refer to the description of the cascade model variant B2 in Müller and Haberlandt (2018).

For the validation the extreme values are extracted as peak-over-threshold to increase the extreme value population due to the shortness of the observed time series (DWA-A 531, 2012). The threshold was chosen in a way to obtain three extreme events per year on average. The independency of the single events is assured by a minimum of 4 h without rainfall between two extreme events. The return periods T of the events are calculated with an empirical distribution function after Fuchs (1983) as suggested in (DWA-A 531, 2012):

$$T = \frac{L + 0.2}{k - 0.4} \frac{M}{L} \tag{2}$$

with k as index of sorted extreme events with 1 for the biggest and L for the smallest event, since L determines the population amount in dependency of the time series length M (with $L = 3$ M).

3.2. Combined sewer system and urban hydrological model

For the representation of the urban hydrology an artificial sewage system is used, which is a common approach to analyse the impacts of rainfall data sets (e.g., Kim and Olivera, 2012). The artificial sewage system used in this study is adopted from Müller and Haberlandt (2018),

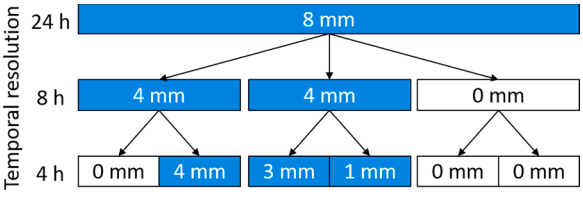

Fig. 3. General scheme of the cascade model for the first two disaggregation steps with exemplary rainfall amounts for a daily total of 8 mm (blue boxes = wet time steps).

and was modified to represent the hydrological characteristics of the study area. The EPA Storm Water Management Model 5.1 (SWMM, Rossman, 2015) was used to simulate the runoff quantity and quality from urban areas simultaneously.

The general setup of the model is explained in the supplementary material S2. Here, we provide details on how we adopted single model parameters for the study area. In total, 22 sub-catchments ranging from 16.5 ha to 240 ha were constructed. The size of the urban hydrological model domain was 2500 ha in total. The widths of the sub-catchments were set according to their actual dimensions ranging from 400 to 3000 m. The surface slopes of the sub-catchments ranged from 1.4–7.3 % with a mean value of 4.1 % according to the respective mean surface elevations of the digital terrain model. The imperviousness of the sub-catchments and the length of the conduits were adjusted during calibration for each sub-catchment so that the timing and duration of simulated and observed CSO discharges matched (calibration results are provided in the supplementary material S2). The imperviousness ranged from 50–100 % (mean value 81 %), and the conduit length ranged from 100–6000 m with a total length of 31.3 km after calibration. A retention tank (40,280 m^3) was implemented to store wastewater mixed with rain water if the capacity of the WWTP is reached. In case of exceedance of the capacity, the water is emitted to the receiving water via CSOs.

Thirty realisations of the disaggregated rainfall time series were applied for each climate scenario period (C20, NTF and LTF). The urban hydrological simulations were run continuously to avoid a priori assumptions about which rainfall extreme values could cause CSOs, and about the soil moisture contents before the rainfall events. This enabled a more realistic simulation of the CSO discharges (Saadi et al., 2020). For simulating the concentrations of enterococci, *Cryptosporidium* and *Giardia* in CSO water, we set the concentrations of the respective parameters in the dry weather flow of raw wastewater (C_{raw}) equal to ten times the mean values observed in raw wastewater at WWTP (Fig. 1, Section 3.4). This was done in order to compensate for the additional contribution of further CSO discharges upstream and diffuse faecal sources via surface runoff in the urban area which were not considered in the artificial sewer system. The respective concentrations in surface runoff were assumed to be zero.

3.3. Rainfall-runoff model

The runoff from the Vienna River catchment was simulated continuously on an hourly time step using a distributed conceptual rainfall-runoff model (Blöschl et al., 2008), which is explained in more detail in the supplementary material S4. The hydrological model domain area is 199 km^2 (Fig. 1). The spatial resolution of the model is 1 km x 1 km. The calibrated and validated hydrological model was used to simulate C20, NTF and LTF. As for the urban hydrological model (Section 3.2), the disaggregated rainfall time series served as model input and were applied as spatial uniform rainfall. Observed air temperature from the meteorological station Hohe Warte during the C20 period served as further model input.

3.4. Dilution of microorganisms in river water and QMRA

The concentrations of microorganisms in CSO water (C_{CSO}, Section 3.2) are diluted with river water downstream the outlet point. The microbial concentration in river water (C_{river}) is calculated as

$$C_{river} = \frac{C_{CSO} \cdot Q_{CSO}}{Q_{river}} + C_{river,\ bg.obs} \tag{4}$$

where Q_{CSO} [m^3/s] is the simulated CSO discharge (Section 3.2), Q_{river} [m^3/s] is the simulated river discharge (Section 3.3), and $C_{river,bg.obs}$ is the microbial background concentration in river water and was described by selected statistical distributions (Section 3.5, more details are provided in the supplementary material S3). Inactivation of

pathogens in the sewer system and in the river directly downstream of the sewage emissions was assumed negligible. Note that future changes in water temperature and the effects of temperature-dependent inactivation also need to be considered when investigating the microbiological river water quality further downstream, as shown e.g. by Sterk et al. (2016).

The risks of infection per person and exposure event are calculated assuming that recreation takes place directly downstream of the sewage emission. The ingested dose D during recreational use is:

$$D = C_{river} \times V \tag{5}$$

where V [m^3] is the individual volume of water that was consumed by swimmers (Schets et al., 2011). V depends on the type of exposure type (i.e. splashing, wading, hand-to-mouth contact of playing children or other visitors, Section 2.1). V is gamma-distributed with values of r = 0.64 and λ=58 for swimming children according to Schets et al. (2011) and Schijven et al. (2015) which is considered a worst-case scenario. To account for the probability of exposure differing over the seasons (Section 2.1), the infection risks are weighted by factors of 0.01 (winter), 0.1 (spring and autumn), and 1 (summer). Alternatively, one could model the likelihood of exposure based on survey data as demonstrated by Sterk et al. (2016). We selected this simplified approach for not introducing another complexity in the model that could mask the effects of climate changes.

For *Cryptosporidium* the risk of infection (P_{inf}) per person and exposure event was calculated using the hypergeometric dose–response model (Teunis and Havelaar 2000):

$$P_{inf} = 1 - {}_1F_1(\alpha, \alpha+\beta, D) \tag{6}$$

where α (0.3) and β (1.1) (Schijven et al., 2015; Schijven et al., 2011) are infectivity parameters that are pathogen-specific and ${}_1F_1$ is the confluent hypergeometric function. For *Giardia* the exponential dose-response model was used (r = 0.02, Regli et al., 1991). The concentrations of enterococci, *Cryptosporidium* and *Giardia* in the river and the risks of infection per person and exposure event for *Cryptosporidium* and *Giardia* were calculated at hourly time steps by solving Eqs. 4–5, and Eq. (6), respectively, for the 30 realisations and the C20, NTF, and LTF periods, respectively.

3.5. Water quality analysis and data

Monthly monitoring for enterococci, and the two reference pathogens *Cryptosporidium* and *Giardia* was conducted of raw wastewater and river water during base flow, and of river water during CSOs and flood events during 2018–2019. The methods and data for sampling and water quality analysis are described in the supplementary material S3.

4. Results

4.1. Rainfall disaggregation

Before the cascade model was applied to disaggregate the rainfall time series for the climate scenarios (C20, NTF, LTF), it was validated for the study area. The performance of the cascade model indicates its applicability for the disaggregation (validation results are provided in the supplementary material S5). The disaggregated rainfall time series were analysed regarding their extreme values with a focus on typical return periods T for urban hydrological applications and dimensioning purposes (T = {2, 5, 10 yrs}). Fig. 4 shows the median rainfall amounts resulting from 30 disaggregation realisations for each GCM – RCM combination and period exemplary for the rainfall durations D = 5 min and D = 2 h, both for return periods T of 2 years. These results are representative for all durations and return periods. Results for rainfall stations P1, P2 and P3 are similar for all D and T, while P5 leads to higher values in all cases. Extreme values for P4 are closer to those for P1, P2 and P3 for D < 1 h and closer to those for P5 for $D \geq 1$ h. Although some of these combinations show an increase for NTF and a decrease for LTF, they show an absolute increase in the future overall. The percent changes of the mean rainfall extreme values are very similar for all stations (see supplementary material S6 for all stations), we therefore discuss the results only for rainfall station P3 (Table 2). Over all return periods and rainfall durations, the rainfall amounts increase by 8–22 % for NTF and 15–33 % for LTF relative to C20 with the largest increases for high return periods and high rainfall durations.

4.2. Hydrological model results

For the results of the urban hydrological model we differentiated between CSO < 1.0 m^3/s, 1 - 1.5 m^3/s and >1.5 m^3/s. The fraction of time steps with CSO increases by 9–39 % relative to C20, with a larger increase for LTF than for NTF (Fig. 5, Table 3). The increase is almost

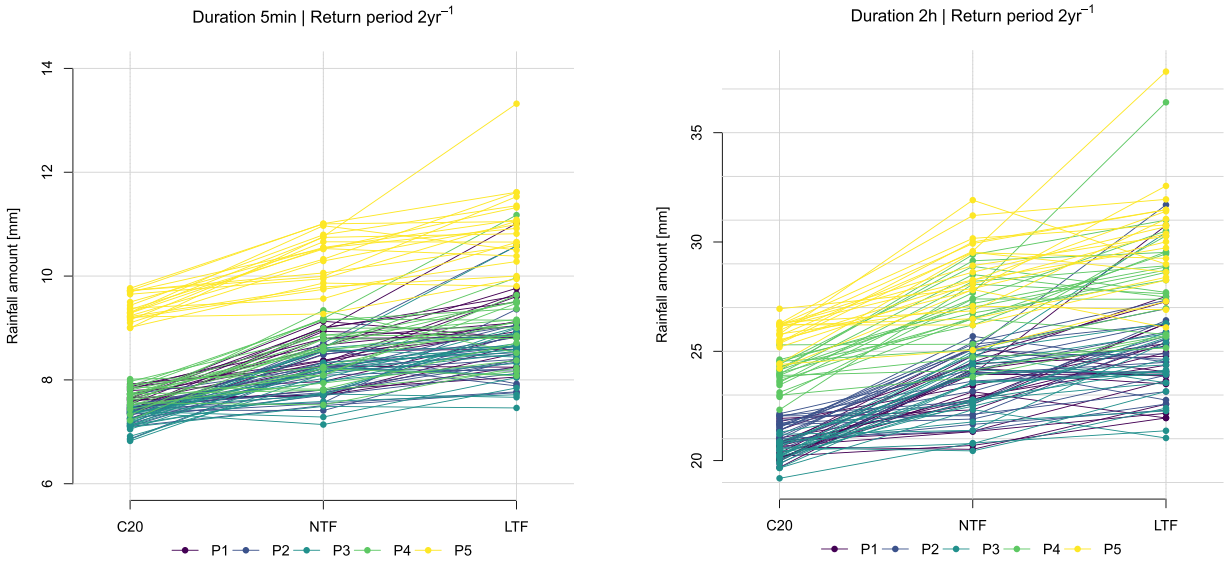

Fig. 4. Rainfall extremes for rainfall stations P1 – P5 with a return period of T = 2 yrs for D={5 min, 2 h}. Each point represents the median of 30 disaggregation realizations.

Table 2
Percent change of rainfall extreme events for NTF and LTF in comparison to C20 for different return periods T and durations D for rainfall station P3.

D	T (yrs)											
	0.33		0.5		1		2		5		10	
	NTF	LTF	NTF	LTF	NTF	LTF	NTF	LTF	NTF	LTF	NTF	LTF
5 min	10	16	10	17	11	19	12	19	14	21	18	24
30 min	10	16	10	17	12	19	13	20	15	23	20	27
1 h	10	16	11	17	12	19	13	20	17	24	21	30
2 h	10	16	11	17	12	19	13	20	17	24	21	30
24 h	8	15	9	16	11	16	11	18	18	22	22	33

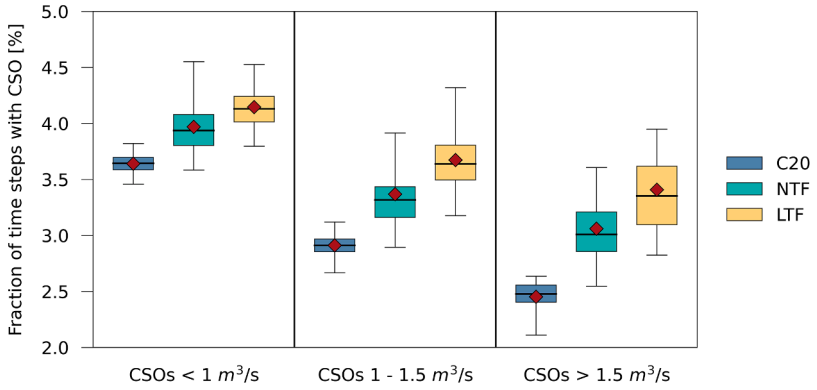

Fig. 5. Fraction of 5 min-time steps during CSO occurrence [%] for the C20, NTF and LTF. CSOs are differentiated for <1.0 m^3/s, 1 - 1.5 m^3/s and >1.5 m^3/s. Red diamonds show the mean, boxes the 25th and 75th percentile, whiskers the 5th and 95th percentile, and black horizontal lines the median values.

Table 3
Fraction of time steps during CSO occurrence [%] followed by the relative change to C20.

Period	Fraction of time steps during CSO occurrence					
	CSO < 1.0 m^3/s		CSO 1 - 1.5 m^3/s		CSO > 1.5 m^3/s	
	Mean value [%]	Relative change to C20 [%]	Mean value [%]	Relative change to C20 [%]	Mean value [%]	Relative change to C20 [%]
C20	3.6	–	2.9	–	2.5	–
NTF	4.0	9	3.4	16	3.1	25
LTF	4.1	14	3.7	26	3.4	39

three times larger for large than for small CSO events (Table 3).

For analysing seasonal effects, we defined all time steps from December to February as winter, all time steps from March to May as spring, all time steps from June to August as summer, and all time steps from September to November as autumn. The simulations showed the highest CSO volumes in summer and the lowest ones in winter for all future periods. For all seasons the simulations showed an increase of CSO volumes by 26 to 37 % for NTF and LTF relative to C20 (Table 4). The future changes in CSO volumes relative to C20 range from 21 to 31 % for NTF, and from 28 to 53 % for LTF over different seasons.

According to the results of the rainfall-runoff model the river runoff is highest in spring, and lowest in autumn in all periods. The river runoff increases relative to C20 by 10 to 19 % for NTF and LTF over all seasons. The relative change to C20 range from 5 to 16 % for NTF, and from 12 to 31 % for LTF over different seasons.

The mean mixing ratio calculated between simulated CSO and river runoff (Q_{cso}/Q_{river}) showed an increase for both NTF and LTF relative to C20 indicating an increase in CSO concentration. As the increases in CSO volumes and river runoff do not linearly correspond, this results in a larger increase of the mixing ratio for NTF (45 %) than for LTF (29 %)

Table 4
Statistics of CSOs, river flows and mixing ratios over the complete simulation time.

Period	Season	CSO		River		Mixing ratio	
		Mean value [m^3/s]	Relative change to C20 [%]	Mean value [m^3/s]	Relative change to C20 [%]	Mean value [-]	Relative change to C20 [%]
C20	**All seasons**	**0.12**	**–**	**2.17**	**–**	**0.036**	**–**
	Winter	0.10	–	1.92	–	0.047	–
	Spring	0.11	–	3.00	–	0.019	–
	Summer	0.15	–	2.25	–	0.035	–
	Autumn	0.12	–	1.48	–	0.042	–
NTF	**All seasons**	**0.15**	**26**	**2.39**	**10**	**0.052**	**45**
	Winter	0.13	31	2.23	16	0.061	30
	Spring	0.14	28	3.14	5	0.033	71
	Summer	0.18	24	2.54	13	0.049	40
	Autumn	0.15	21	1.62	10	0.065	53
LTF	**All seasons**	**0.17**	**37**	**2.57**	**19**	**0.046**	**29**
	Winter	0.15	53	2.51	31	0.061	30
	Spring	0.16	38	3.37	12	0.027	39
	Summer	0.19	28	2.62	16	0.042	18
	Autumn	0.16	35	1.77	20	0.055	31

relative to C20 over all seasons.

4.3. Microbiological river water quality and infection risks during recreational use

The dilution of microorganisms in river water (Section 3.4) resulted in mean concentrations of enterococci, *Cryptosporidium* and *Giardia* of 7.0×10^4 CFU/l, 7.4 oocysts/l and 28.8 cysts/l for C20 in the river downstream of the sewage emissions from CSOs over all seasons (Table 5). The mean infection risks during recreational use (i.e. splashing, wading, hand-to-mouth contact of playing children and other visitors) are 1.25 % and 0.47 % per person and exposure event for *Cryptosporidium* and *Giardia*, respectively, according to the QMRA (Table 6).

The seasonal analysis for C20 showed that the mean concentrations are highest in autumn and lowest in spring, i.e. on average 10 / 20 % higher and 10 / 40 % lower than over all seasons for *Cryptosporidium* / *Giardia*, respectively (Table 5). In contrast, the mean infection risks are highest in summer and lowest in winter, i.e. on average 230 % higher and 100 % lower than over all seasons (Table 6). This is mainly attributed to the fact that the assumed likelihood of exposure is highest and lowest during these seasons, respectively (Section 3.4). The infection risks for *Cryptosporidium* and *Giardia* increase relative to C20, with lowest increases in summer (e.g. 33 % for NTF and LTF for *Giardia*), and highest increases in spring (47 and 38 % for *Giardia*, Table 6). For *Cryptosporidium*, the infection risks increase only by 7–10 % in the future. This is because in contrast to concentrations of enterococci and *Giardia*, which were by factors of 39 and 7 higher in the river during CSOs than during base flow, concentrations of *Cryptosporidium* were by a factor of 2 lower (results not shown). To investigate the 95th percentile infection risks, we evaluated the cumulative probabilities for *Giardia* (Fig. 6). The 95th percentile infection risks range from 0.08 % in winter to 8 % per person and exposure event in summer for C20, and increase by 0.2–0.3 $\log_{10}$ in the future. The 95th percentile infection risk was also used to evaluate the variability resulting from different climate scenarios, seasons and disaggregation realizations. The variability of infection risks was higher over different seasons than over different climate scenarios and rainfall disaggregation realizations (ranging over up to 2.4, 0.8 and 0.1 $\log_{10}$ % per person and exposure event, respectively, Fig. 7). The infection risks increase by up to 0.8 $\log_{10}$ in the future for individual scenarios (Fig. 7 left).

For evaluating the microbiological water quality model, we compared the simulated concentrations of enterococci, *Cryptosporidium* and *Giardia* in the river for C20 (Table 5) with the measured concentrations in the river during CSOs and flood events in 2018–2021 (see supplementary material S2). For this comparison, we considered the mean simulated values for C20 over the time steps when CSOs occurred. According to that the observed and simulated concentrations matched with mean errors of 0.10–0.15 $\log_{10}$ CFU/l or (oo)cysts/l.

Table 6
Mean *Cryptosporidium* and *Giardia* infection risks [%] per person and exposure event during recreational use of river water calculated over 30 years of simulation time for C20, NTF and LTF with rainfall time series from 21 different regional climate models applied from station P3.

Period	Season	*Cryptosporidium*		*Giardia*	
		Infection risk [%]	Relative change to C20 [%]	Infection risk [%]	Relative change to C20 [%]
C20	**All seasons**	**1.25**	–	**0.47**	–
	Winter	0.04	–	0.02	–
	Spring	0.38	–	0.10	–
	Summer	4.13	–	1.56	–
	Autumn	0.42	–	0.17	–
NTF	**All seasons**	**1.35**	**8**	**0.62**	**34**
	Winter	0.04	7	0.02	32
	Spring	0.41	8	0.15	47
	Summer	4.44	7	2.07	33
	Autumn	0.45	9	0.23	36
LTF	**All seasons**	**1.35**	**8**	**0.62**	**34**
	Winter	0.04	8	0.02	35
	Spring	0.41	6	0.14	38
	Summer	4.44	7	2.07	33
	Autumn	0.46	10	0.24	41

5. Discussion

In this study, we presented a novel probabilistic-deterministic modelling approach for quantifying the effect of climate change on the microbiological river water quality considering recreational water safety downstream of sewage emissions from CSOs. This approach allows for the first time addressing this question considering the predictive uncertainty of short-term rainfall events by a physically plausible generation of future rainfall time series at sub-daily time scales. This is an important consideration because the relative change of the extreme values on the daily scale in general does not represent the relative change of extreme values on finer temporal scales. This was shown before by e.g. Burn and Taleghani (2013), and Bürger et al. (2021), and also in our simulations. For return periods of 0.33 years, e.g., the future increase in extreme rainfall values relative to C20 was found similar for durations of 5 min as for durations of one day. In contrast, for return periods of 10 years, the relative change in extreme rainfall values

Table 5
Mean concentrations of enterococci [CFU/l], *Cryptosporidium* [oocysts/l] and *Giardia* [cysts/l] in river water calculated over 30 years of simulation time for C20, NTF and LTF with rainfall time series from 21 different regional climate models applied from station P3.

Period	Season	enterococci [CFU/l]	Relative change to C20 [%]	*Cryptosporidium* [oocysts/l]	Relative change to C20 [%]	*Giardia* [cysts/l]	Relative change to C20 [%]
C20	**All seasons**	$\mathbf{7.0 \times 10^4}$	**–**	**7.4**	**–**	**28.8**	**–**
	Winter	8.0×10^4	–	7.7	–	32.7	–
	Spring	4.3×10^4	–	6.6	–	18.4	–
	Summer	7.3×10^4	–	7.5	–	30.0	–
	Autumn	8.4×10^4	–	7.8	–	34.1	–
NTF	**All seasons**	$\mathbf{9.1 \times 10^4}$	**31**	**8.1**	**9**	**37.1**	**29**
	Winter	9.9×10^4	24	8.3	8	40.2	23
	Spring	6.2×10^4	45	7.2	9	25.8	40
	Summer	9.0×10^4	23	8.0	7	36.5	21
	Autumn	1.1×10^5	37	8.8	12	46.1	35
LTF	**All seasons**	$\mathbf{8.6 \times 10^4}$	**24**	**7.9**	**7**	**35.2**	**22**
	Winter	1.0×10^5	25	8.4	8	40.5	24
	Spring	5.5×10^4	30	7.0	6	23.2	26
	Summer	8.3×10^4	14	7.8	4	34.1	13
	Autumn	1.1×10^5	28	8.6	9	43.1	26

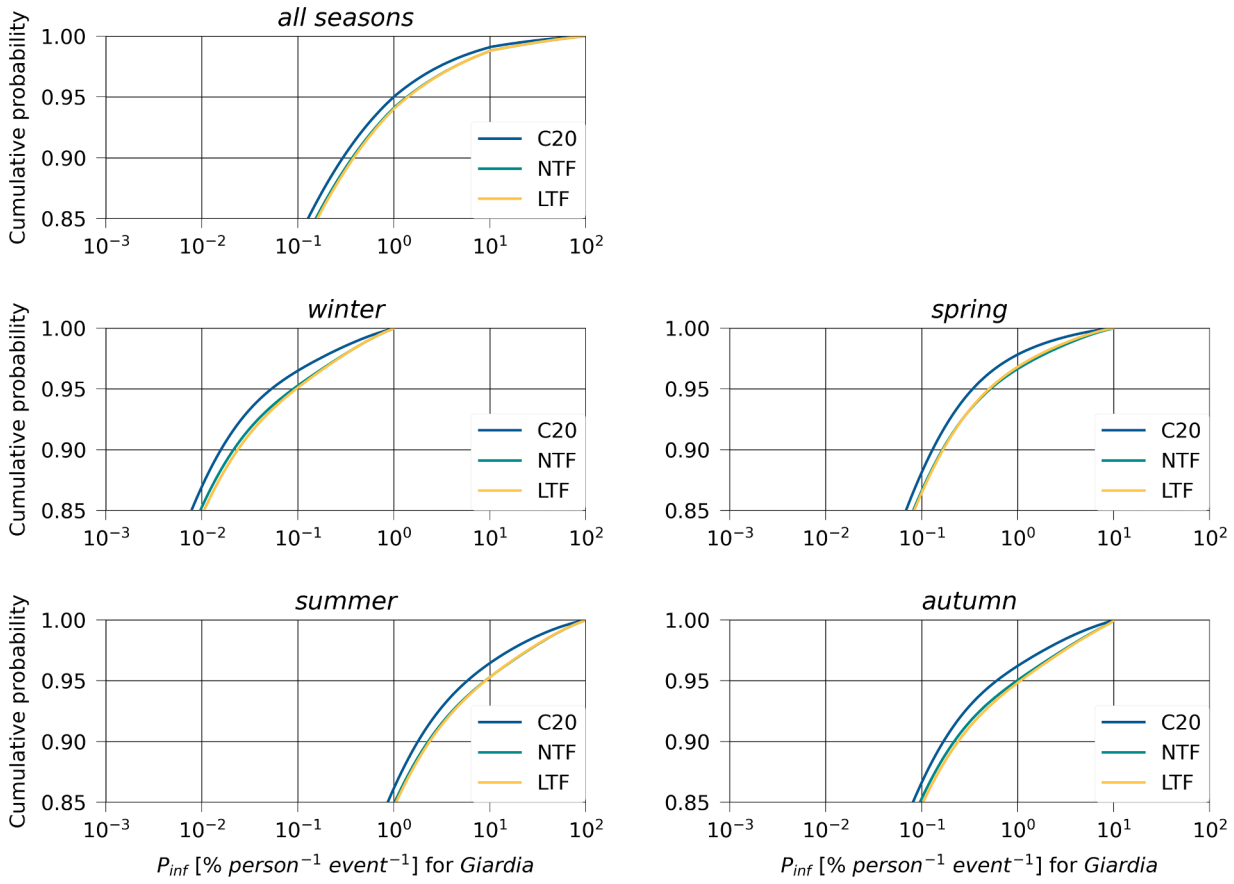

Fig. 6. Cumulative probability distributions of the upper percentile infection risks [% per person and exposure event] for *Giardia* during recreational use in the river downstream of sewage emissions from CSOs over 30 years of simulation time for C20, NTF and LTF with rainfall time series from 21 different regional climate models applied from station P3.

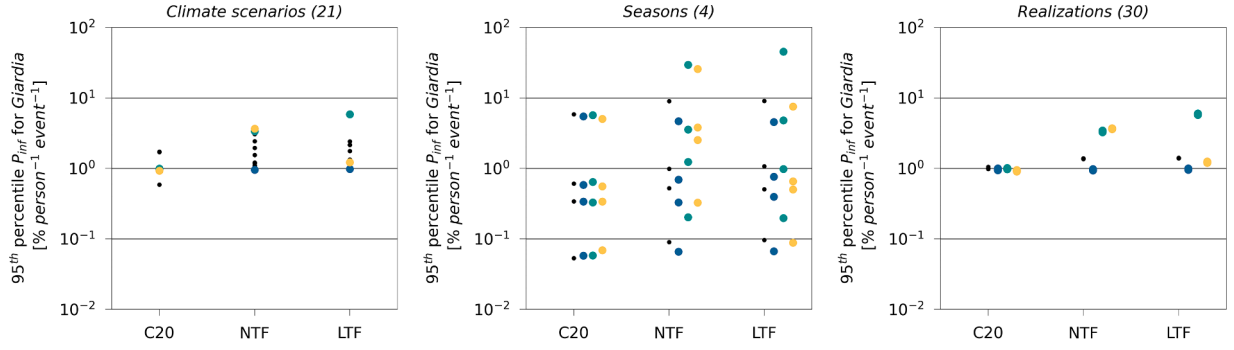

Fig. 7. Variability of 95th infection risks [% per person and exposure event] for *Giardia* resulting from different climate scenarios (left), seasons (centre) and disaggregation realizations (right). Shown are averages over all climate scenarios (black), and values for three selected climate scenarios (blue, green, yellow).

between future and reference periods was 10–11 % smaller for durations of 5 min than for durations of one day. Our simulation results reflected the ability of the enhanced micro-canonical cascade by Müller and Haberlandt (2018) to account for the physical characteristics of the rainfall time series during disaggregation; i.e., while more frequent rainfall extreme values result rather from strong convective and hence short-duration events, less frequent rainfall extremes originate from stratiform events with a more homogeneous temporal distribution of rainfall amounts.

The model simulations revealed that higher ranges of climate change effects on the infection risks downstream of sewage emissions are possible (up to 0.8 $\log_{10}$) than previously shown due to the range of considered climate models (e.g. Abdellatif et al., 2015, Sterk et al., 2016). On top of that, the simulations revealed strong variations in infection risks over seasons and different climate scenarios, ranging over 2.4 and 0.8 $\log_{10}$ % per person and exposure event, respectively. Uncertainties with regards to climate models and emission scenarios arise regarding how the human population will develop in the upcoming decades but also due to mathematical simplifications, phenomena which are not yet completely understood such as storm trains, or longer droughts, or the natural variability of the climate systems (Chimani et al., 2018). All climate models and assumptions have the same justification, and to account for their intrinsic climate variability and model uncertainty, it is best to include many of them in the climate analyses (Chimani et al., 2018; Martre et al., 2015). This inclusion demands a statistical downscaling of the climate scenario time series as suggested in

this study, which is faster and less computationally intense than a physical downscaling. A physical downscaling of all climate scenarios is to date not feasible.

There are further global change factors affecting the river water quality downstream of sewage emissions from CSOs which were not considered in this study. The climate warming and associated increase of evaporation can have an impact on urban runoff and CSOs. This effect is, however, presumably small in urban areas due to the limited storage. Moreover, the changes of evaporation partly depend on vegetation dynamics, which are not well reflected in current climate scenario runs. Future adaptation measures such as the implementation of green infrastructure adds to the complexity of this question. These effects could be subject of future research particularly for the analysis of seasonal changes of future river water quality downstream sewage emissions from CSOs. Studying these effects, however, would require a bias-correction of regional climate models for precipitation and future temperature data at sub-daily temporal scale. Future research on climate change with regards to water quality and safety must focus further on characterizing the impacts of climate change at a local scale (Jalliffier-Verne et al. 2017), e.g. by employing spatial downscaling techniques for regional climate models, or by including enhanced observation data of CSOs.

The presented approach can further be used for characterizing the microbiological water quality based on the simulated concentrations of faecal indicators in the river. For our study site, e.g., the simulated mean concentrations of enterococci in the river (Table 4) correspond with the microbiological water quality assessment category D and $a > 10$ % risk of GI illness according to the WHO guidelines on recreational water quality (WHO, 2021). Note, however, that the recreational activities at our study site (i.e. splashing, wading, hand-to-mouth contact of playing children and other visitors), lead in general to lower exposure than during swimming. Also, with the presented approach the seasonal variation of exposure can be accounted for e.g. according to Sterk et al. (2016).

The integrated approach presented in this study can be applied in other urban river settings by using site-specific historic rainfall time series at high temporal resolution and regional climate models. Ideally, a calibrated urban hydrological model should be used instead of an artificial sewer network. While demonstrated here for enterococci, and the protozoan reference pathogens *Cryptosporidium* and *Giardia,* the model approach can be extended for any other pathogen. The approach can aid in supporting the sustainable urban water safety planning, and the selection of appropriate infection protection measures.

6. Conclusions

This study presents a novel probabilistic-deterministic modelling approach for predicting the future changes in the microbiological river water quality considering safe recreational use downstream of sewage emissions from CSOs. Building on the enhanced micro-canonical cascade by Müller and Haberlandt (2018), the approach allows for the first time evaluating this question by use of continuous rainfall time series at sub-daily temporal resolution. The demonstrated approach allows considering a multitude of regional climate scenarios and the uncertainty of generated future rainfall time series resulting in probabilistic distribution ranges of all predicted variables. The model simulations revealed strong variations in infection risks over seasons and different climate scenarios, ranging over 2.4 and 0.8 $\log_{10}$ % per person and exposure event, respectively. The increase of infection risks in the future is 0.2–0.3 $\log_{10}$ per person and exposure event over the ensemble of 21 ÖKS15-projections and up to 0.8 $\log_{10}$ % per person and exposure event for individual climate scenarios. Investments to prevent CSOs would be beneficial to ensure sustainable recreational water safety. In future studies the presented approach could be adopted to other emerging pathogens and contaminants and aid in evaluating the effectiveness of mitigation measures such as the implementation of green infrastructure or the unsealing of paved areas.

Declaration of Competing Interest

The authors declare that they have no known competing financial interests or personal relationships that could have appeared to influence the work reported in this paper.

Data availability

The authors are unable or have chosen not to specify which data has been used.

Acknowledgements

First of all, Damien Batstone as associated editor and two anonymous reviewers are gratefully acknowledged. Their suggestions and comments helped to improve the manuscript significantly. This study was supported by the Vienna Science and Technology Fund (WWTF) [10.47379/ESR17070] with research project no. ESR17-070, by the research project Vienna Water Resource Systems 2020+ (ViWa2020+), in cooperation with the City of Vienna (Vienna Water, MA31) and the SwimCity project with research project no. JF_2019_15 funded by the Austrian Academy of Science. We thank the Vienna City Administration Wien Kanal for providing information on the sewer system and the precipitation data, and the Vienna City Administration MA45 for providing the river discharge data. Hannes Müller-Thomy acknowledges the funding from the Research Fellowship (MU 4257/1-1) by DFG e.V., Bonn, Germany. We thank Dr. Juraj Parajka for his feedback to the discussion on the uncertainty with regards to climate models.

Supplementary materials

Supplementary material associated with this article can be found, in the online version, at doi:10.1016/j.watres.2023.120746.

References

Abdellatif, M., Atherton, W., Alkhaddar, R., Osman, Y., 2015. Quantitative assessment of sewer overflow performance with climate change in northwest England. Hydrol. Sci. J. 60 (4), 636e650. https://doi.org/10.1080/02626667.2014.912755.

Berg, P., Moseley, C., Haerter, J.O., 2013. Strong increase in convective precipitation in response to higher temperatures. Nat. Geosci. 6, 181–185. https://doi.org/10.1038/NGEO1731.

Blöschl, G., Reszler, C., Komma, J., 2008. A spatially distributed flash flood forecasting model. Environ. Model. Softw. 23 (4), 464–478. https://doi.org/10.1016/j.envsoft.2007.06.010.

Breinl, K., Di Baldassarre, G., 2019. Space-time disaggregation of precipitation and temperature across different climates and spatial scales. J. Hydrol., Region. Stud. 21, 126–146. https://doi.org/10.1016/j.ejrh.2018.12.002.

Bürger, G., Pfister, A., Bronstert, A., 2021. Zunehmende Starkregenintensitäten als Folge der Klimaerwärmung: Datenanalyse und Zukunftsprojektion. Hydrol. und Wasserbewirtschaftung 65 (6), 262–271. https://doi.org/10.5675/HyWa_2021.6_1.

Burn, D.H., Taleghani, A., 2013. Estimates of changes in design rainfall values for Canada. Hydrol. Process. 27 (11), 1590–1599. https://doi.org/10.1002/hyp.9238.

Cardona, O.D., van Aalst, M.K., Birkmann, J., Fordham, M., McGregor, G., Perez, R., Pulwarty, R.S., Schipper, E.L.F., Sinh, B.T., 2012. Determinants of risk: exposure and vulnerability. In: Field, C.B., Barros, V., Stocker, T.F., Qin, D., Dokken, D.J., Ebi, K.L., Mastrandrea, M.D., Mach, K.J., Plattner, G.-K., Allen, S.K., Tignor, M., Midgley, P.M. (Eds.), Managing the Risks of Extreme Events and Disasters to Advance Climate Change Adaptation. A Special Report of Working Groups I and II of the Intergovernmental Panel on Climate Change (IPCC). C.U.P, Cambridge, UK, and New York, NY, USA, pp. 65–108.

CCCA, 2020. Climate Change Centre Austria. https://ccca.ac.at/startseite.

Chimani, B., Matulla, C., Eitzinger, J., Hiebl, J., Hofstätter, M., Kubu, G., Maraun, D., Mendlik, T., Schellander-Gorgas, T., Thaler, S., 2018. Guideline zur Nutzung der ÖKS15-Klimawandelsimulationen sowie der entsprechenden gegitterten Beobachtungsdatensätze. Manual (in German).

Christensen, J.H., Christensen, O.B., 2003. Severe summertime flooding in Europe. Nature 421, 805–806. https://doi.org/10.1038/421805a.

DeSilva, M.B., Schafer, S., Kendall Scott, M., Robinson, B., Hills, A., Buser, G.L., Salis, K., Gargano, J., Yoder, J., Hill, V., Xiao, L., Roellig, D., Hedberg, K., 2016. Communitywide cryptosporidiosis outbreak associated with a surface water-supplied

municipal water system–Baker City, Oregon, 2013. Epidemiol. Infect. 144 (2), 274–284. https://doi.org/10.1017/s0950268815001831.
DWA-A 531, 2012. Starkregen in Abhängigkeit von Wiederkehrzeit und Dauer. Technical guideline of the DWA. Hennef.
Feng, Y., Xiao, L., 2011. Zoonotic potential and molecular epidemiology of *Giardia* species and Giardiasis. Clin. Microbiol. Rev. 24 (1), 110–140. https://doi.org/10.1128/cmr.00033-10.
Gogien, F., Dechesne, M., Martinerie, R., Lipeme Kouyi, G., 2022. Assessing the impact of climate change on Combined Sewer Overflow based on small time step future rainfall timeseries and long-term continuous sewer network modelling. Water Res. https://doi.org/10.1016/j.watres.2022.119504.
Gooré Bi, E., Monette, F., Gachon, P., Gaspéri, J., Perrodin, Y., 2015. Quantitative and qualitative assessment of the impact of climate change on a combined sewer overflow and its receiving water body. Environ. Sci. Pollut. Res. 22 (15), 11905–11921. https://doi.org/10.1007/s11356-015-4411-0.
Guzman, H., Bernardo, R., Freiesleben de Blasio, B., MacDonald, E., Nichols, G., Sudre, B., Vold, L., Semenza, J.C., Nygård, K., 2015. Analytical studies assessing the association between extreme precipitation or temperature and drinking water-related waterborne infections: a review. Environ. Health 14, 29. https://doi.org/10.1186/s12940-015-0014-y.
Jalliffier-Verne, I., Leconte, R., Huaringa-Alvarez, U., Madoux-Humery, A.S., Galarneau, M., Servais, P., Prévost, M., Dorner, S., 2015. Impacts of global change on the concentrations and dilution of combined sewer overflows in a drinking water source. Sci. Total Environ. 508, 462–476. https://doi.org/10.1016/j.scitotenv.2014.11.059.
Jalliffier-Verne, I., Leconte, R., Huaringa-Alvarez, U., Heniche, M., Madoux-Humery, A. S., Autixier, L., Galarneau, M., Servais, P., Prévost, M., Dorner, S., 2017. Modelling the impacts of global change on concentrations of Escherichia coli in an urban river. Adv Water Resour. 108, 450–460. https://doi.org/10.1016/j.advwatres.2016.10.001.
Kim, D., Olivera, F., 2012. Relative importance of the different rainfall statistics in the calibration of stochastic rainfall generation models. J. Hydrol. Eng. 17 (3), 368–376. https://doi.org/10.1061/%28ASCE%29HE.1943-5584.0000453.
Koutsoyiannis, D., Onof, C., 2001. Rainfall disaggregation and adjusting procedures on a Poisson cluster model. J. Hydrol. 246, 109–122. https://doi.org/10.1016/S0022-1694(01)00363-8.
Martre, P., Wallach, D., Asseng, S., Ewert, F., Jones, J.W., Rötter, R.P., Boote, K.J., Ruane, A.C., Thorburn, P.J., Cammarano, D., Hatfield, J.L., Rosenzweig, C., Aggarwal, P.K., Angulo, C., Basso, B., Bertuzzi, P., Biernath, C., Brisson, N., Challinor, A.J., Doltra, J., Gayler, S., Goldberg, R., Grant, R.F .HL., Hooker, J., Hunt, L.A., Ingwersen, J., Izaurralde, R.C., Kersebaum, K.C., Müller, C., Kumar, S.N., Nendel, C., O'Leary, G., Olesen, J.E., Osborne, T.M., Palosuo, T., Priesack, E., Ripoche, D., Semenov, M.A., Shcherbak, I., Steduto, P., Stöckle, C.O., Stratonovitch, P., Streck, T., Supit, I., Tao, F., Travasso, M., Waha, K., White, J.W., Wolf, J., 2015. Multimodel ensembles of wheat growth: many models are better than one. Glob. Change Biol. 21 (2), 911–925. https://doi.org/10.1111/gcb.12768.
MDDEFP, 2013. Ministère du Développement Durable, de l'Environnement, de la Faune et des Parcs du Québec (2013) Critères de Qualité De L'eau De Surface, 3e édition, 510. Direction du suivi de l'état de l'environnement, Québec, p. 16. ISBN 978-2-550-68533-3.
Müller, H., Haberlandt, U., 2015. Temporal rainfall disaggregation with a cascade model: from single-station disaggregation to spatial rainfall. J. Hydrol. Eng. 20 (11) https://doi.org/10.1061/(ASCE)HE.1943-5584.0001195.
Müller, H., Haberlandt, U., 2018. Temporal rainfall disaggregation using a multiplicative cascade model for spatial application in urban hydrology. J. Hydrol. 556, 847–864. https://doi.org/10.1016/j.jhydrol.2016.01.031.
Müller-Thomy, H., 2019. Improving the autocorrelation in disaggregated time series for urban hydrological applications, P. In: Peleg, N., Molnar, P. (Eds.), 11th Workshop On Precipitation in Urban Areas (UrbanRain18). Pontresina, Switzerland, pp. 75–76. https://doi.org/10.3929/ethz-b-000347485.
Müller-Thomy, H., 2020. Temporal rainfall disaggregation using a micro-canonical cascade model: possibilities to improve the autocorrelation. Hydrol. Earth Syst. Sci. 24, 169–188. https://doi.org/10.5194/hess-24-169-2020.
Ochoa-Rodriguez, S., Wang, L.P., Gires, A., Pina, R.D., Reinoso-Rondinel, R., Bruni, G., Ichiba, A., Gaitan, S., Cristiano, E., van Assel, J., Kroll, S., Murlà-Tuyls, D., Tisserand, B., Schertzer, D., Tchiguirinskaia, I., Onof, C., Willems, P., ten Veldhuis, M.C., 2015. Impact of spatial and temporal resolution of rainfall inputs on urban hydrodynamic modelling outputs: a multi-catchment investigation. J. Hydrol. 531 (2), 389–407. https://doi.org/10.1016/j.jhydrol.2015.05.035.
Olsson, J., 1998. Evaluation of a scaling cascade model for temporal rainfall disaggregation. Hydrol. Earth Syst. Sci. 2 (1), 19–30. https://doi.org/10.5194/hess-2-19-1998.
Peel, M.C., Finlayson, B.L., McMahon, T.A., 2007. Updated world map of the Köppen-Geiger climate classification. Hydrol. Earth Syst. Sci. 11, 1633–1644. https://doi.org/10.5194/hess-11-1633-2007.
Regli, S., Rose, J.B., Haas, C.N., Gerba, C.P., 1991. Modeling the risk from *Giardia* and viruses in drinking-water. J. Am. Water Works Assoc. 83 (11), 76–84. https://doi.org/10.1002/j.1551-8833.1991.tb07252.x.
Rossmann, L.A., 2015. Storm Water Management Model User's manual Version 5.1. Environmental Protection Agency, U.S.
Saadi, M., Oudin, L., Ribstein, P., 2020. Beyound imperviousness: the role of antecedent wetness in runoff generation in Urbanized catchments. Water Resour. Res. 65 (11), e2020WR028060 https://doi.org/10.1029/2020WR028060.
Schets, F.M., Schijven, J.F., Husman, A.M.D., 2011. Exposure assessment for swimmers in bathing waters and swimming pools. Water Res. 45 (7), 2392–2400. https://doi.org/10.1016/j.watres.2011.01.025.
Schijven, J., Derx, J., Husman, A.M.D., Blaschke, A.P., Farnleitner, A.H., 2015. QMRAcatch: microbial quality simulation of water resources including infection risk assessment. J. Environ. Qual. 44 (5), 1491–1502. https://doi.org/10.2134/jeq2015.01.0048.
Schijven, J.F., Teunis, P.P.M., Rutjes, S.A., Bouwknegt, M., Husman, A.M.D., 2011. QMRAspot: a tool for quantitative microbial risk assessment from surface water to potable water. Water Res. 45 (17), 5564–5576. https://doi.org/10.1016/j.watres.2011.08.024.
Schilling, W., 1991. Rainfall data for urban hydrology: what do we need? **Atmos. Res.** 27 (1–3), 5–21. https://doi.org/10.1016/0169-8095(91)90003-F.
Semenza, J.C., 2020. Cascading risks of waterborne diseases from climate change. Nat. Immunol. 21, 484–487. https://doi.org/10.1038/s41590-020-0631-7.
Sterk, A., de Man, H., Schijven, J.F., de Nijs, T., Husman, A.M.D., 2016. Climate change impact on infection risks during bathing downstream of sewage emissions from CSOs or WWTPs. Water Res 105, 11–21. https://doi.org/10.1016/j.watres.2016.08.053.
Taylor, K.E., Stouffer, R.J., Meehl, G.A., 2012. An overview of CMIP5 and the experiment design. Bull. Am. Meteorolog. Soc. 93, 485–498. https://doi.org/10.1175/BAMS-D-11-00094.1.
Teunis, P.F., Havelaar, A.H., 2000. The Beta Poisson dose-response model is not a single-hit model. Risk Anal. 20 (4), 513–520. https://doi.org/10.1111/0272-4332.204048.
Trenberth, K.E., 2011. Changes in precipitation with climate change. Clim. Res. 47 (1), 123–138. https://doi.org/10.3354/CR00953.
WHO, 2021. Guidelines on recreational water quality. In: Coastal and Fresh Waters, Volume 1. World Health Organization, p. 164. ISBN: 978-92-4-003130-2.